

A Simple and Accurate Formula for Oscillating Amplitude of CMOS LC Differential Oscillator

Nikorn Hen-ngam* and Jirayuth Mahatanakul**, Non-members

ABSTRACT

The conventional formula for the oscillation amplitude of the CMOS LC differential oscillator was derived under the assumption that the current from sourced coupled pair flowing through LC tank is a square wave. This is not in line with the real situation and the obtained formula is independent of the MOSFET parameters. In this paper, a derivation of a simple and accurate expression for oscillating amplitude of CMOS LC differential oscillator in which the current from sourced coupled pair is assumed to be clipped sinusoid is presented. By comparing to the simulation results, it was found that the new expression of oscillating amplitude is more accurate than the widely used conventional expression.

Keywords: Amplitude, Oscillator.

1. INTRODUCTION

Oscillation amplitude is one of the important parameters of an oscillator. For a local oscillator (LO) in the transceiver, phase noise, which is the ratio between the power of main oscillation amplitude and sideband noise (see Fig. 1), is one of the key parameters in wireless telecommunication system. The effect of phase noise in downconversion process in RF transceiver is illustrated in Fig. 2 where the wanted signal is corrupted by the interferer even though they are in different frequency bands [1].

Fig. 3 shows the widely used LC CMOS oscillator, which is composed of cross-coupled MOS source coupled pair and LC tank. The resistance $r_s/2$ is the parasitic element associated with the losses in the inductor. Together with phase noise and power consumption, the oscillation amplitude is one of the most important specifications for a local oscillator employed in RF applications. The oscillator in Fig. 3 provides sinusoidal voltage

$$V_{osc}(t) = V_p \sin(2\pi f_{osc}t + \theta) \quad (1)$$

Manuscript received on January 20, 2015 ; revised on March 24, 2015.

* The author is with Department of Information Technology, Faculty of Industrial Technology, Ubon Ratchathani Rajabhat University, Ubon Ratchathani, Thailand, E-mails: nikoro_h@hotmail.com.

** The author is with Department of Electronics Engineering, Mahanakorn University of Technology Nongchok, Bangkok, Thailand, E-mails: jirayuth@mut.ac.th

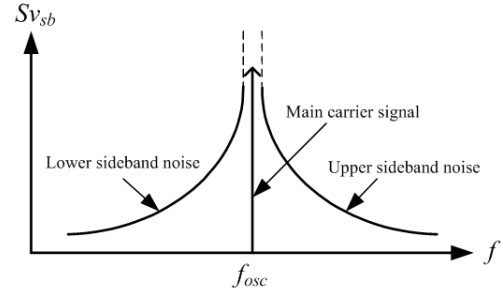


Fig. 1: Spectrum of the voltage signal from an actual oscillator.

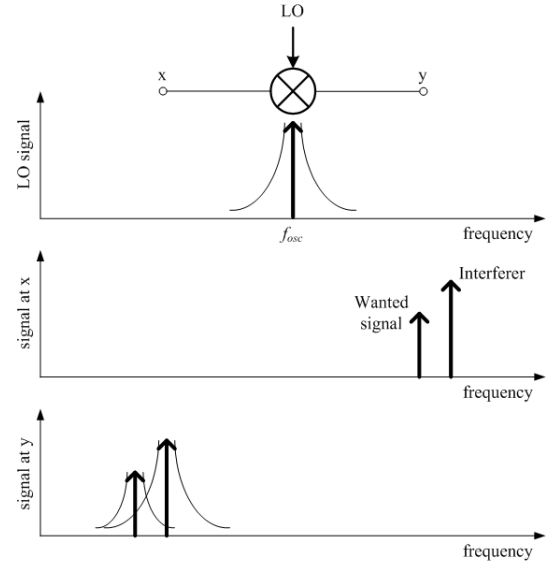


Fig. 2: Downconversion by mixing the RF signal with a LO signal.

$$f_{osc} = \frac{1}{2\pi\sqrt{L_s C}} \quad (2)$$

is the oscillation frequency and V_p is the oscillation amplitude whose expression is conventionally given as [2-5]

$$V_p = \frac{2I_{ss}L_s}{\pi r_s C} \quad (3)$$

However according to (3) the value of V_p is independent of the MOSFET device parameters, which

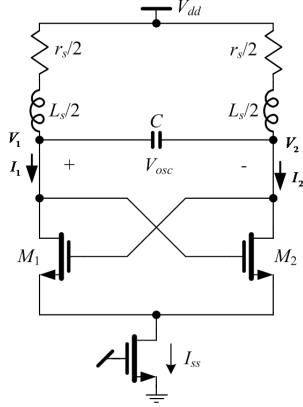


Fig.3: CMOS cross-coupled differential oscillator.

does not reflect the real situation. In this paper, the more accurate expression of V_p will be derived and the results compared with the simulation results.

2. DIFFERENTIAL MODE ANALYSIS OF SUBCIRCUITS IN CMOS DIFFERENTIAL OSCILLATOR

The oscillator in Fig. 3 can be divided into two parts, i.e. the LC tank and the cross-coupled CMOS network. In this section, the differential-mode (DM) half circuits of these subcircuits will be derived. Fig. 4(a) shows LC tank in the oscillator in Fig. 3. According to differential-mode (DM) analysis in the Appendix, the DM half circuit of LC tank in Fig. 4(a) is shown in Fig. 4(b) where

$$V_D = V_1 - V_2 \text{ and } I_D = I_1 - I_2$$

By performing ac analysis, the impedance of DM LC tank in Fig. 4(b) can be found to be

$$Z_a(f) = \frac{j2\pi f L_s/2 + r_s}{(j2\pi f)^2 L_s C + j2\pi f C r_s + 1} \quad (4)$$

However, at frequencies close to oscillation frequency, f_{osc} , Z_a is equation (4) can be approximated as

$$Z_a(f) \approx \frac{j2\pi f L_s/2}{(j2\pi f)^2 L_s C + j2\pi f C r_s + 1} \quad (5)$$

By rearranging Eq. (5), we obtain

$$Z_a(f) \approx \frac{1}{j2\pi f_{osc} C/2 + \frac{1}{j2\pi f_{osc} L_s/2} + \frac{1}{R_L/2}} \quad (6)$$

where

$$R_L = \frac{L_s}{r_s C} \quad (7)$$

which corresponds to the LRC parallel network in Fig. 4(c).

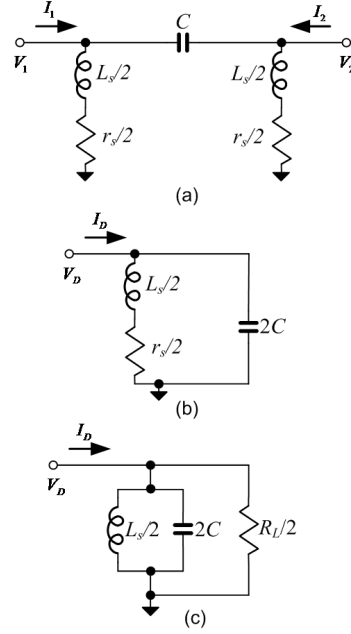


Fig.4: (a) LC tank used in Fig. 3 (b) DM half circuit of the LC tank in (a) (c) Parallel RLC tank

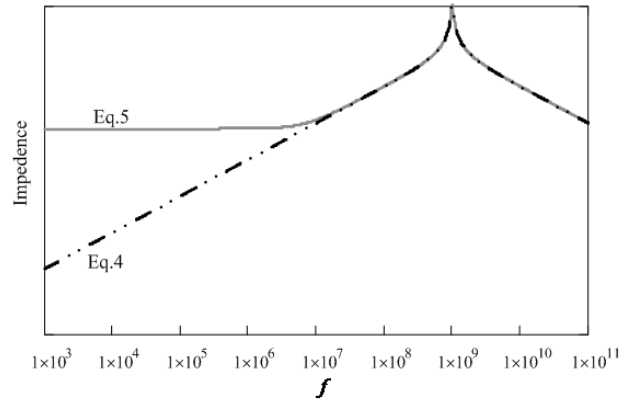


Fig.5: AC responses of impedance functions in Eq. (4) and (5) where $L_s = 12.6\text{nH}$, $C = 2\text{pf}$ and $r_s = 4.41\ \Omega$.

As shown in Fig. 5, the impedances of the LC networks in Fig. 4(b) and (c) are almost identical to each other at frequencies close to oscillation frequency. [6] By using MOSFET square law, the relationship between DM input voltage and DM output current,

$$V_D = V_1 - V_2 \text{ and } I_D = I_1 - I_2$$

of the CMOS sourced coupled pair in Fig. 6 can be described by the following equation [7],

$$I_D = \begin{cases} -I_{ss} & ; \quad V_D < -V_s \\ g_m V_D \sqrt{1 - \left(\frac{V_D g_m}{2I_{ss}}\right)^2} & ; \quad -V_s < V_D < V_s \\ I_{ss} & ; \quad V_D > V_s \end{cases} \quad (8)$$

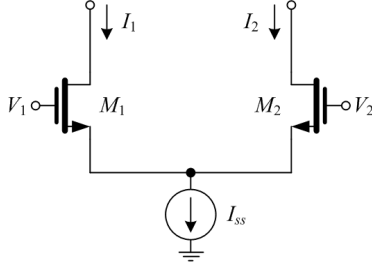


Fig.6: CMOS source coupled pair.

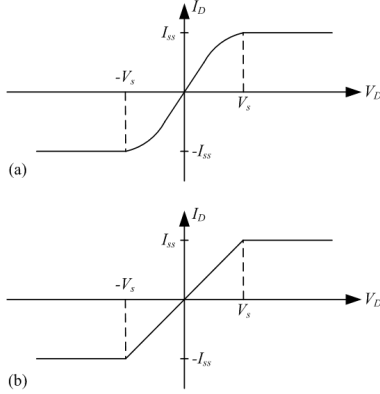


Fig.7: (a) DM I-V curve of CMOS source coupled pair (b) Piecewise-linear approximation of the curve in (a).

where

$$V_s = \sqrt{\frac{2I_{SS}}{\mu_n C_{ox}(W/L)}} \quad (9)$$

and

$$g_m = \sqrt{I_{SS}\mu_n C_{ox}(W/L)} \quad (10)$$

However in the following analysis the piecewise-linear curve in Fig. 7(b) will be used in preference to the curve in Fig. 7(a). This is necessary otherwise the analysis will become too complicated and we would not be able to find the closed-form solution for the oscillation amplitude.

Fig. 8(a) shows the cross-coupled sourced coupled pair network employed in the oscillator in Fig. 3. By comparing the circuit of Fig. 8(a) to that of Fig. 6(a), the large-signal DM half circuit of Fig. 8(a) can be obtained as shown in Fig. 8(b).

3. OSCILLATION AMPLITUDE CALCULATION

According to Fig. 4 and 8 from the previous section, the DM half circuit of the differential CMOS oscillator in Fig. 3 can be illustrated in Fig. 9.

Since the upper and lower parts in Fig 9 are connected in parallel, the circuit in Fig. 9 can be redrawn to emphasize this as shown in Fig. 10.

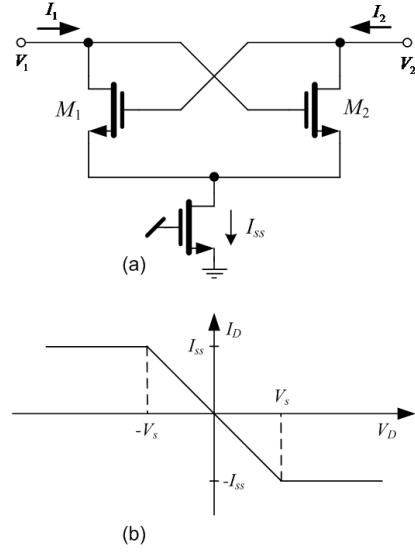


Fig.8: (a) Cross-coupled source coupled pair in Fig. 3 (b) I-V characteristic of the circuit in (a) .

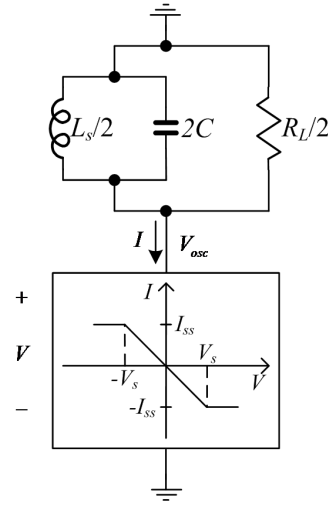


Fig.9: DM half-circuit of the oscillator in Fig.3.

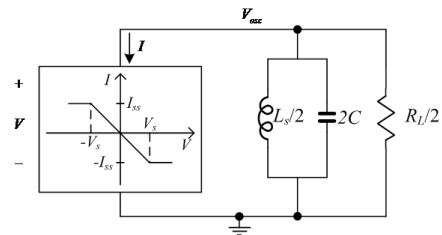


Fig.10: The circuit in Fig. 9 redrawn to emphasize parallel connection between the top and bottom parts.

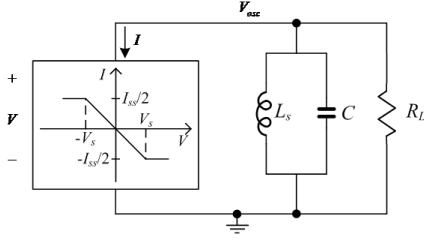


Fig.11: The circuit of Fig. 10 after scaling.

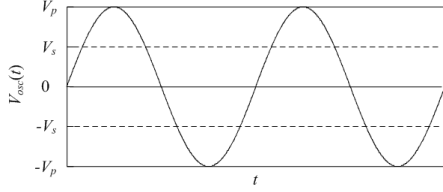


Fig.12: The waveform of V_{osc} in Fig. 11.

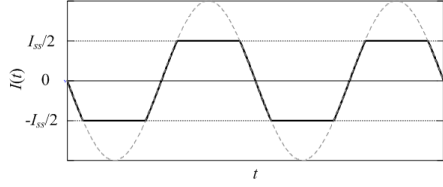


Fig.13: The waveform of I in Fig. 11.

Referring to Fig. 10, if we scale up the value of the impedance of the RLC parallel network and scale down the I-V curve of the block in the left hand side by the same factor, the value of V_{osc} will be the same. By performing such scaling with the scaling factor of two (such that the inductance, resistance and capacitance become L_s , R_L and C respectively), we obtain the circuit in Fig. 11.

According to Fig. 11, the relationship between V_{osc} and I can be described by the equation,

$$I(t) = \begin{cases} \frac{-I_{ss}}{2V_m} V_{osc}(t) & ; |V_{osc}(t)| < V_s \\ \frac{I_{ss}}{2} & ; V_{osc}(t) < -V_s \\ \frac{-I_{ss}}{2} & ; V_{osc}(t) > V_s \end{cases} \quad (11)$$

Therefore if the oscillating voltage V_{osc} is pure sinusoidal (Fig. 12), the waveforms of the current I can be shown in Fig. 13.

3.1 Conventional Expression

Conventional expression of the oscillation amplitude in equation (3) can be obtained by assuming that the wave form of the current I is a square wave as shown in Fig. 14. [5]

By employing Fourier analysis, the current I in Fig. 14 can be broken down into two components as

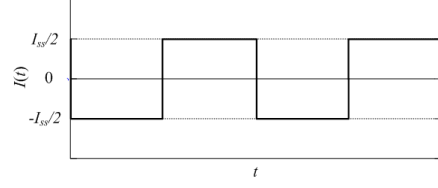


Fig.14: The waveform of I when approximated as a square wave.

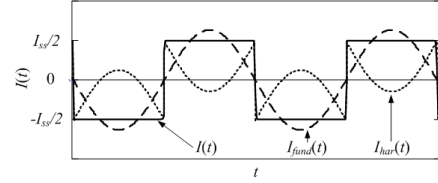


Fig.15: The waveforms of $I(t)$, $I_{fund}(t)$ and $I_{har}(t)$.

$$I(t) = I_{fund}(t) + I_{har}(t) \quad (12)$$

where

$$I_{fund}(t) = \frac{2I_{ss} \sin \omega_{osc} t}{\pi} \quad (13)$$

and

$$I_{har}(t) = \frac{2I_{ss}}{\pi} \left[\frac{\sin 3\omega_{osc} t}{3} + \frac{\sin 5\omega_{osc} t}{5} + \dots \right] \quad (14)$$

The waveforms of I_{fund} and I_{har} are shown in Fig. 15. At oscillation frequency $\omega_{osc} = 2\pi f_{osc}$, the impedance of LC is infinity and thus the fundamental current I_{fund} would not flow into the LC network at all. As a result, the current I_{fund} would flow only into R_L causing V_{osc} to be sinusoidal with amplitude [2-5]

$$V_p = \frac{2I_{ss}R_L}{\pi} \quad (15)$$

By substituting (7) into (15), we have

$$V_p = \frac{2I_{ss}I_s}{\pi r_s C} \quad (16)$$

However according to (16), the value of V_p is independent of the MOSFET device parameters, which should not be the case. In the next subsection, a more accurate expression of V_p will be derived and the results will be compared with the simulation results

3.2 New Expression

Referring to Fig. 13, according to Fourier series analysis, the current I , which is a clipped sinusoidal,

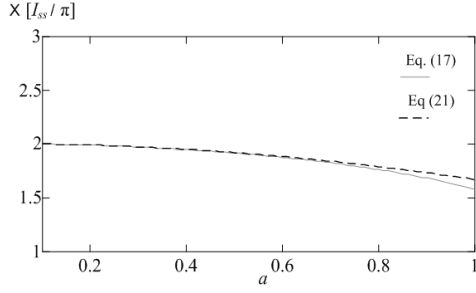


Fig.16: Plots of Equations (17) and (21).

is composed of fundamental element at frequency f_{osc} and infinite number of harmonic elements. The magnitude of such a fundamental element can be found as

$$I_{fund} = \left(\frac{a\sqrt{1-a^2} + \sin^{-1} a}{a} \right) \frac{I_{ss}}{\pi} \quad (17)$$

where

$$a = \frac{V_s}{V_p} \quad (18)$$

Now since a is always less than unity, we can use the following Taylor series approximations

$$\sqrt{1-a^2} = 1 - \frac{a^2}{2} \quad (19)$$

and

$$\sin^{-1}(a) \cong a - \frac{a^3}{6} \quad (20)$$

to approximate equation (17) as

$$I_{fund} \cong \left(2 - \frac{a^2}{3} \right) \frac{I_{ss}}{\pi} \quad (21)$$

It can be observed from Fig. 16 that equation (21) is a very good approximation of equation (17) until variable a is higher than about 0.8. Since the impedance of LC parallel network at f_{osc} is infinite, the fundamental element of the current I would flow only through RL producing V_{osc} with amplitude

$$V_p = I_{fund} R_L \quad (22)$$

Substituting (21) into (22) gives

$$V_p = \left(2 - \frac{a^2}{3} \right) \frac{I_{ss} R_L}{\pi} \quad (23)$$

It should be noted that in the case where V_s is much smaller than V_p , the variable $a = V_s/V_p$ will become small and equation (23) can be reduced to

$$V_p = \frac{2I_{ss} R_L}{\pi} \quad (24)$$

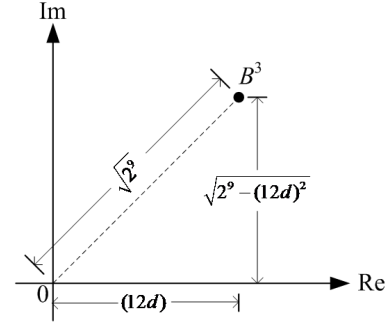


Fig.17: Geometric representation of variable B^3 in the complex plane.

By substituting (7) into (24), we have

$$V_p = \frac{2I_{ss} I_s}{\pi r_s C} \quad (25)$$

which is the same as the conventional expression in equation (16).

Now by substituting (18) into (23) and rearranging the results, we obtain the cubic equation

$$\frac{a^3}{3} - 2a + d = 0 \quad (26)$$

where

$$d = \frac{\pi V_s}{I_{ss} R_L} \quad (27)$$

By solving (26), we have

$$a = \frac{B}{4} + \frac{2}{B} + j\sqrt{3}\left(\frac{B}{4} - \frac{2}{B}\right) \quad (28)$$

where for

$$d < (2^9/144)^{1/2} = 1.886 \quad (29)$$

B is a complex entity and can be expressed as (see Fig. 17 for the plot of B^3 in complex plane)

$$B = \left[12d + j\sqrt{2^9 - (12d)^2} \right]^{1/3} \quad (30)$$

It can be observed from Fig. 17 that the magnitude of B^3 is

$$|B^3| = \sqrt{2^9} \quad (31)$$

and thus

$$|B|^2 = \left(\sqrt{2^3} \right)^2 = 8 \quad (32)$$

By substituting the above equation to the identity equation

$$|B|^2 = BB^* \quad (33)$$

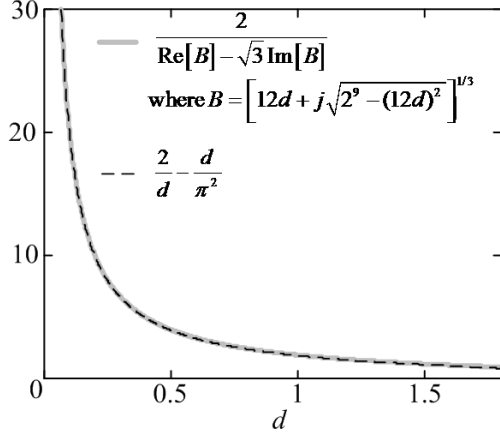


Fig.18: Plots of the left-hand side and right-hand side of equation (38).

and rearranging the result, we have

$$\frac{2}{B} = \frac{B^*}{4} \quad (34)$$

Substituting (34) into (28) gives

$$a = \frac{B + B^*}{4} + j\sqrt{3} \left(\frac{B - B^*}{4} \right) \quad (35)$$

Then by using the identities

$$\frac{B+B^*}{2} = \text{Re}[B] \text{ and } \frac{B-B^*}{2} = j\text{Im}[B]$$

equation (35) can be re-written as

$$a = \frac{\text{Re}[B] - \sqrt{3}\text{Im}[B]}{2} \quad (36)$$

By substituting (36) into (18) we have

$$V_p = \frac{2V_s}{\text{Re}[B] - \sqrt{3}\text{Im}[B]} \quad (37)$$

According to Fig. 18 we found that

$$\frac{2}{\text{Re}[B] - \sqrt{3}\text{Im}[B]} \cong \frac{2}{d} - \frac{d}{\pi^2} \quad (38)$$

and thus by substituting (38) into (37), we have

$$V_p \cong \left(\frac{2}{d} - \frac{d}{\pi^2} \right) V_s \quad (39)$$

Substituting (9) into (39) gives

$$V_p = \left(\frac{2}{d} - \frac{d}{\pi^2} \right) \sqrt{\frac{2I_{SS}}{\mu_n C_{ox}(W/L)}} \quad (40)$$

Lastly by substituting (27) into (40) and rearranging the result, we obtain

$$V_p = \frac{2I_{SS}L_s}{\pi r_s C} - \frac{2r_s C}{\pi \mu_n C_{ox}(W/L)L_s} \quad (41)$$

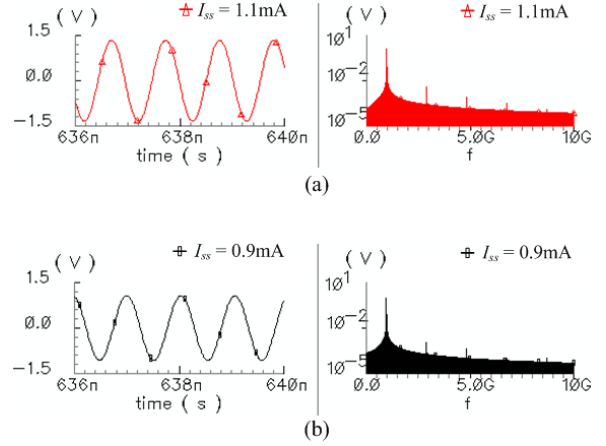


Fig.19: Simulated waveforms and FFT of the V_{osc} of Fig 3 where $W/L = 35\mu\text{m}/2\mu\text{m}$ for (a) $I_{SS} = 1.1\text{mA}$ and (b) $I_{SS} = 0.9\text{mA}$.

By comparing (41) to the conventional expression in (16), it can be found that the value of V_p in (41) is less than the conventional expression by

$$V_{diff} = \frac{2r_s C}{\pi \mu_n C_{ox}(W/L)L_s} \quad (42)$$

which is dependent upon values of MOS parameters and passive elements.

4. SIMULATION RESULTS

By using the 0.35 micron AMS CMOS technology process parameters, the oscillator of Fig. 1 was designed to have oscillation frequency of 1 GHz. The designed oscillators were simulated with Virtuoso Spectre and the simulation results are shown in Fig. 19 and 20

It can be observed from Fig. 20(a) that the oscillating amplitude is dependent upon the bias current I_{SS} and the simulation results are in better agreement with the derived expression in equation (41) than the conventional expression in equation (16). However from Fig. 20(b), we can see that the derived expression will not give accurate results when $d < 1.886$ which is the lower limit for d (see (29)).

5. CONCLUSION

In this paper, the CMOS LC differential oscillator is analyzed and the new expression of oscillating amplitude is derived. The derived expression in equation (41) contains a term that is dependent on the MOS-FET device parameters, which is not the case for the conventional expression in equation (16). It can be observed from Fig. 20 that when compared to the simulation result, the derived expression is found to be much more accurate than the conventional expression.

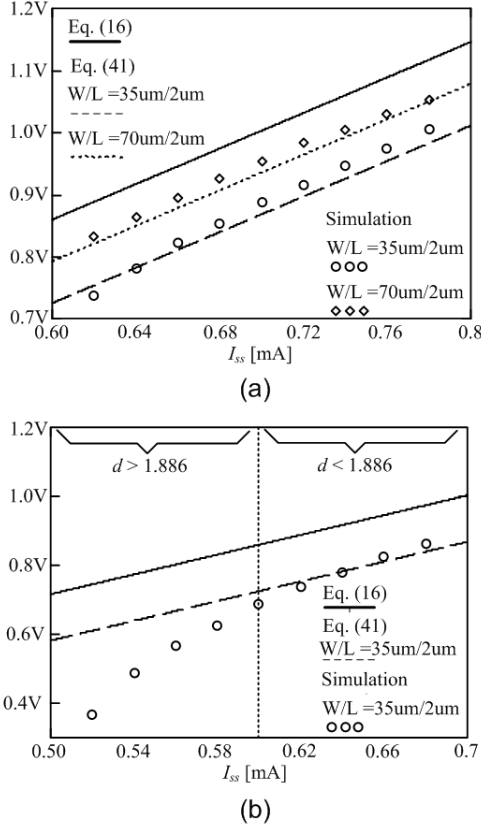


Fig.20: The oscillation amplitude of the oscillator in Fig. 3 along with the analytical results Eq. (16) and (41) where $\mu_n C_{ox} = 0.12 \text{ mA/V}^2$

APPENDIX

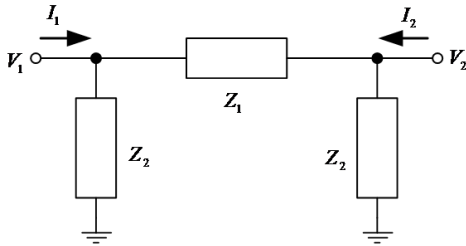


Fig.21: Analyzed network.

Referring to Fig. 21, the currents I_1 and I_2 can be found to be

$$I_1 = \frac{V_1}{Z_2} + \frac{V_1 - V_2}{Z_1} \quad (43)$$

and

$$I_2 = \frac{V_2}{Z_2} + \frac{V_2 - V_1}{Z_1} \quad (44)$$

respectively. If the DM voltage and DM current are conventionally defined as

$$V_D = V_1 - V_2 \quad (45)$$

and

$$I_D = I_1 - I_2 \quad (46)$$

respectively. Substituting (43) and (44) into (46) yields

$$I_D = \frac{V_1 - V_2}{Z_2} + \frac{V_1 - V_2}{Z_1/2} \quad (47)$$

Then by substituting (45) into (47), we obtain

$$I_D = \frac{V_D}{Z_2} + \frac{V_D}{Z_1/2} \quad (48)$$

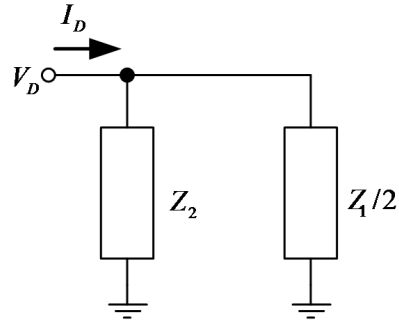


Fig.22: DM Half circuit of the network in Fig. A1.

According to equation (48), the DM half circuit of the network in Fig. 21 can be illustrated in Fig. 22.

References

- [1] B. Razavi, "RF Microelectronics," Englewood Cliffs, NJ: Prentice, 1997.
- [2] A. Abidi, J. Rael, and E. Hegazi, "The designer's guide to high-purity oscillators," Kluwer Academic Publishers, New York, 2005.
- [3] A. Hajimiri and T. H. Lee, "A general theory of phase noise in electrical oscillators," *IEEE J. Solid State Circuits*, vol. SC-33, no.2, pp. 179-194, Feb. 1998.
- [4] A. Hajimiri and T. H. Lee, "Phase noise in CMOS differential LC oscillators," in *IEEE Proc. VLSI Circuits*, 1998, pp. 48-51.
- [5] C. Samori, A. L. Lacaita, F. Villa, and F. Zappa, "Spectrum folding and phase noise in LC tuned oscillators," *IEEE Trans. Circuits Syst. II: Analog Digital Signal Process.*, vol. 45, no.7, pp. 781-790, 1998.
- [6] B. Razavi, "Design of Analog CMOS integrated circuits," MacGraw-Hill, 2001.
- [7] D. Johns and K. Martin, "Analog integrated circuit design," Wiley, New York, 1997.



Nikorn Hen-ngam received the B.S. degree in Physics from Chiang Mai University in 2006, Thailand, and M.E degree in Electrical Engineer, major in Electronics, from Mahanakorn University of Technology in 2009, Thailand. Currently, he is studying a doctorate in Electrical Engineer at Mahanakorn University of Technology. His research interest includes the analysis of phase noise in sinusoidal oscillator.



Jirayuth Mahatanakul received the B.Eng. degree from King Mongkut's Institute of Technology Ladkrabang, Bangkok, Thailand, in 1990, the M.S. degree from Florida Institute of Technology, USA, in 1992, and the Ph.D. degree from Imperial College London, United Kingdom, in 1998, all in electrical engineering. From 1992 to 1994, he was with True Corporation in the Network Planning and Engineering Division.

Since 1994, he joined Mahanakorn University of Technology, Bangkok, Thailand where he is currently a Vice Rector for Academic Affairs.